

probably exposed to pressures considerably in excess of 700 kbar.

Diamond from Dyalpur shows no preferred orientation. One could suggest that the diamonds in this meteorite were formed by gravitational pressure rather than by shock as in Goalpara and Novo Urei. However, Dyalpur's textural similarity to the other two ureilites (particularly to Novo Urei (16) would argue against different modes of diamond formation by Occam's principle (see 17).

Figure 3 (a, b, and c) shows certain features which may have bearing on the details of shock formation of diamond in Goalpara. First, some degree of asymmetry seems evident in the distribution of groupings in each set of normals. Second, there are two "nodes" in the [220] that occur at about 20°. The former effect may be explained by lattice distortion of the diamond crystallites while the latter may be due to the presence of some diamonds formed by rarefaction waves or by secondary shocks. Another feature which may be of significance is that there appear to be only a few groupings at about 51°. These angles occur three times within the crystal (multiplicity III) and should be more prominent than the 63° angle which occurs twice (multiplicity II). This effect may only be an apparent one inasmuch as the zones in the Goalpara [311] are quite extended and markedly overlap the 51° line. The only other reasonable match for the groupings would be by planes parallel to the (220). Were these the oriented planes, however, we would not expect the group at about 30° in the [220] or at about 60° in the [111]. It is possible that the observed distribution of axes is due to some combination of oriented (110) and (311) planes, although the available evidence favors the interpretation of the oriented planes being parallel to (311) only.

From an examination of meteoritic and artificially shock-produced diamonds some suggestions can be made concerning the mechanism of conversion of graphite to diamond by shock. At pressures well below 300 kbar, polycrystalline fine-grained diamond is apparently formed from polycrystalline graphite, possibly by the compression of rhombohedral graphite only (4). From pressures of about 300 kbar to well above 700 kbar the solid-state reaction involves conversion of the basal (001) plane of graphite to diamond (311), or possibly some combination of (311) and (110). Only at

very high pressures may the conversion involve the hypothetical "metallic carbon" postulated by Libby (18) or possibly formation from shock-melted graphite.

The simultaneous presence of graphite, diamond, and kamacite in all of the ureilitic "diamonds" that I have investigated shows that these grains are not equilibrium assemblages. This raises the question of whether they represented an arrested stage in the conversion of graphite to diamond, or vice versa. Studies at 0 kbar (19) and 100 kbar (20) show that graphite formed from diamond shows preferred orientation. In at least two meteorites, however, it is the diamonds which are oriented, and in all diamantiferous meteorites the graphite is polycrystalline and randomly oriented. Thus, the graphite cannot have been formed from diamond. On the other hand, the theory predicts that, under favorable circumstances, shock-formed diamond would show preferential orientation. It thus appears that all meteoritic diamonds were formed by shock rather than by gravitational compression of graphite.

MICHAEL E. LIPSCHUTZ\*

U.S. Army, Goddard Space Flight Center, Greenbelt, Maryland

#### Reference and Notes

1. M. E. Lipschutz and E. Anders, *Geochim. Cosmochim. Acta* **24**, 83 (1961).
2. ———, *Science* **134**, 2095 (1961).
3. E. C. T. Chao, E. M. Shoemaker, B. M. Madsen, *ibid.* **132**, 220 (1960); E. C. T. Chao, J. Fahey, J. Littler, D. Milton, *J. Geophys. Res.* **67**, 419 (1962).
4. P. DeCarli and J. Jamieson, *Science* **133**, 1821 (1961).
5. Major minerals in these meteorites are olivine, (Mg, Fe)<sub>2</sub>SiO<sub>4</sub>, and clinopyroxene, (Ca, Mg, Fe) SiO<sub>3</sub>. The meteorites contain, in addition, minor amounts of diamond, graphite, kamacite ( $\alpha$ -iron), troilite (FeS), and chromite (FeCr<sub>2</sub>O<sub>4</sub>). No other stony meteorites are known to contain diamond although well over 260 others have been examined for diamond by various investigators.

6. E. Anders, *Astrophys. J.* **134**, 1006 (1961).
7. Unicam Instruments Ltd., Cambridge, England.
8. N. F. M. Henry, H. Lipson, W. A. Wooster, *The Interpretation of X-Ray Diffraction Photographs* (Macmillan, New York, ed. 2, 1961), Fig. 108.
9. A. Taylor, *X-Ray Metallography* (Wiley, New York, 1961), Fig. 258.
10. H. C. Urey, A. Mele, T. Mayeda, *Geochim. Cosmochim. Acta* **13**, 1 (1957).
11. *International Tables for X-Ray Crystallography* (Kynock, Birmingham, England, 1959), vol. 2.
12. H. W. Fairbairn, *Structural Petrology of Deformed Rocks* (Addison-Wesley, Cambridge, Mass., ed. 2, 1949).
13. H. L. Pugh, J. Lees, J. A. Bland, *Nature* **191**, 865 (1961); J. A. Kohn and D. W. Eckart, *Am. Mineralogist* **47**, 1422 (1962); H. O. A. Meyer and H. J. Milledge, *Nature* **199**, 167 (1963).
14. F. P. Bundy, *J. Chem. Phys.* **38**, 631 (1963).
15. D. S. Hughes and R. G. McQueen, *Trans. Am. Geophys. Union* **39**, 959 (1958).
16. L. G. Kwascha, *Chem. Erde* **19**, 249 (1958).
17. Since this paper was submitted, A. P. Vinogradov and G. P. Vdovkin [*Geokhimiya* No. 8, 715 (1963)] have independently confirmed the presence of diamond in the three ureilites. In addition, they have announced the discovery of diamond in yet another stony meteorite, Ghubara. When samples of this meteorite can be obtained, the properties of Ghubara's diamonds and olivine can be compared with those of the ureilites.
18. W. F. Libby, *Proc. Natl. Acad. Sci. U.S.A.* **48**, 1475 (1962).
19. H. J. Grenville-Wells, *Mineral. Mag.* **29**, 803 (1952).
20. V. M. Titova and S. I. Futergendler, *Soviet Phys. Cryst. (English Transl.)* **7**, 749 (1963).
21. M. E. Lipschutz, *Science* **138**, 1266 (1962).
22. M. Yerofeyev and P. Lachinov, *Compt. Rend.* **196**, 1679 (1888).
23. I am very grateful to Edward Anders for his many suggestions and comments during the course of this investigation. I also thank John Jamieson and Paul S. DeCarli, for many stimulating discussions, and E. C. T. Chao for his comments on the thin sections of the meteorites. I gratefully acknowledge the loan of the Dyalpur meteorite (E. Olsen, Chicago Natural History Museum) and the Goalpara and Novo Urei meteorites and thin sections (E. P. Henderson, U.S. National Museum). Gifts of synthetic diamonds produced by various techniques were received from R. H. Wentorf, Jr. (General Electric Research Laboratory), M. Waxman (National Bureau of Standards), and P. S. DeCarli (Stanford Research Institute). Miss Vida Milanovic and Miss Donna Reichel provided valuable assistance. The Materials Research and Development Section, NASA, lent equipment during the course of this research, which was supported in part by National Science Foundation grant G 14298.

\* Present address: Physikalisches Institut, Universität Bern, Sidlerstrasse 5, Bern, Switzerland.

28 January 1964

## Mössbauer Effect for Surface Atoms: Iron-57 at the Surface of $\eta$ Al<sub>2</sub>O<sub>3</sub>

Abstract. *The Mössbauer effect has been observed for Fe<sup>57</sup> atoms at the surface of  $\eta$  Al<sub>2</sub>O<sub>3</sub>. The Fe<sup>57</sup> is trivalent, and the quadrupole splitting found is consistent with a surface location. Anisotropy of thermal vibration relative to the surface is observed.*

The Mössbauer effect offers a promising means of investigating both the electronic structure and the lattice dynamics of atoms at surfaces. The availability of materials with very large ratios of surface to volume makes it possible to prepare specimens whose

surfaces contain large numbers of atoms showing this effect. Relatively conventional techniques of physical chemistry show that the atoms of interest are actually on the surface. For example, studies of the catalysis of *ortho-to-para* conversion in hydrogen have shown that

when alumina is properly impregnated with iron under oxidizing conditions, most of the iron remains on the surface of the alumina (1).

We prepared a sample of  $\eta$   $\text{Al}_2\text{O}_3$  (2) with  $\text{Fe}^{57}$  ions in surface sites. Pure bayerite ( $\beta$   $\text{Al}_2\text{O}_3 \cdot 3\text{H}_2\text{O}$ ) was converted to  $\eta$   $\text{Al}_2\text{O}_3$  by heating at  $250^\circ\text{C}$  for 16 hours, which was then calcined at  $500^\circ\text{C}$  for 16 hours. The specific surface area of the alumina after this treatment was  $340 \text{ m}^2/\text{g}$ . The  $\text{Fe}^{57}$  was applied by the incipient wetness method; 3 mg of 91 percent enriched  $\text{Fe}^{57}$  in HCl solution was used to wet 250 mg of the  $\eta$   $\text{Al}_2\text{O}_3$ , which was then dried at  $120^\circ\text{C}$  and again calcined at  $500^\circ\text{C}$  for 16 hours.

The Mössbauer resonance spectrum was measured with constant velocity apparatus (3). The spectra obtained at room temperature and at  $77^\circ\text{K}$  are shown in Fig. 1. Several features are clear: (i) The patterns are centered about approximately  $0.45 \text{ mm/sec}$ , indicating that the iron atoms are in the  $\text{Fe}^{3+}$  state (4). (ii) There is a relatively large quadrupole splitting, indicating that the iron nuclei are in a highly asymmetrical electrical environment. (iii) The heights of the two peaks of the doublet differ appreciably at room temperature, as a result of anisotropy of the amplitude of thermal vibration (5).

These observations are in qualitative, and rough quantitative, agreement with what one might expect. Since the specimen was prepared under oxidizing conditions, the absence of  $\text{Fe}^{2+}$  is not surprising. We may make a rough calculation of the quadrupole splitting as follows. The normal  $\text{Fe}^{3+}$  site in  $\eta$   $\text{Al}_2\text{O}_3$  is octahedral; we will regard an  $\text{Fe}^{3+}$  ion in a surface site as missing one  $\text{O}^-$  nearest neighbor and estimate the electric-field gradient at the iron nucleus as that due to a charge of  $+2$  at the normal oxygen neighbor distance. We neglect the effects of the removal of more distant neighbors. For a charge  $2e$  at a distance  $r$ , the electric-field gradient seen by a nucleus is:

$$\frac{\partial^2 V}{\partial Z^2} = (1 - \gamma_\infty) \frac{2e}{r^3} \quad (1)$$

where  $(1 - \gamma_\infty)$  is the Sternheimer anti-shielding term (6).

The observed splitting  $\Delta\nu$  is then given by:

$$\Delta\nu = 2\epsilon \frac{c}{E} = \frac{4e}{r^3} (1 - \gamma_\infty) Q \frac{c}{E} \quad (2)$$

where  $\epsilon$  is the splitting,  $c$  is the velocity of light,  $E$  is the energy of the gamma

ray, and  $Q$  is the nuclear quadrupole moment. There is, unfortunately, some uncertainty in the numerical value of the product  $(1 - \gamma_\infty)Q$ . The value of  $\gamma_\infty$  has been calculated for  $\text{Fe}^{3+}$  by Burns (7), but it is difficult to estimate precisely how reliable such calculations are. Values of  $Q$  ranging from 0.12 barn (8) to 0.4 barn (7) have been reported. Probably the best value for our purposes is 0.28 barn for  $\text{Fe}^{3+}$  in solution in  $\text{Al}_2\text{O}_3$  given by Wertheim and Buchanan (9), together with Burns' value of  $\gamma_\infty = -6.18$ , since their experiment involved essentially the same product of  $(1 - \gamma_\infty)Q$ . This choice results in a calculated value of  $1.6 \text{ mm/sec}$  for  $\Delta\nu$ , which does not differ seriously from our experimental results (Table 1).

There is no temperature dependence of the splitting. This is reasonable, since the mechanism giving rise to a temperature dependence (10) should be absent for  $\text{Fe}^{3+}$  ions. We also note that the sign of the quadrupole interaction is positive, so that the upper peak arises from the  $3/2$  level of the excited state. This fact is important in interpreting the anisotropic Debye-Waller factor.

The relative intensities of the transitions to the  $3/2$  and  $1/2$  levels of the excited state, denoted by  $I_{3/2}$  and  $I_{1/2}$ , respectively, are given by:

$$I_{3/2}(\theta) = I_0 \langle \exp - i(\boldsymbol{\kappa} \cdot \mathbf{X}) \rangle^2 (1 + \cos^2 \theta) \quad (3)$$

$$I_{1/2}(\theta) = I_0 \langle \exp - i(\boldsymbol{\kappa} \cdot \mathbf{X}) \rangle^2 \left( \frac{2}{3} - \cos^2 \theta \right)$$

where  $\boldsymbol{\kappa}$  is the wave vector of the gamma ray,  $\mathbf{X}$  is the displacement vector of the active atom, and  $\theta$  is the angle between the principal axis of the electric-field gradient tensor and the direction of observation.

If we assume a random orientation of particles and introduce the harmonic approximation, and substitute  $u$  for  $\cos \theta$ , the ratio of intensities can be reduced to:

$$R = \frac{I_{3/2}}{I_{1/2}} = \frac{\int_0^1 (1 + u^2) \exp(-\epsilon u^2) du}{\int_0^1 \left(\frac{2}{3} - u^2\right) \exp(-\epsilon u^2) du} \quad (4)$$

$$\epsilon = \kappa^2 (\langle z^2 \rangle - \langle x^2 \rangle)$$

where  $\langle z^2 \rangle$  and  $\langle x^2 \rangle$  are the mean square amplitudes of vibration parallel and perpendicular, respectively, to the principal axis of the electric-field gradient tensor. We have evaluated the integrals in Eq. 4 numerically;  $R$  as a function of  $\epsilon$  is plotted in Fig. 2. In our experiment, at  $300^\circ\text{K}$ ,  $R$  is approximately 0.94, so that  $\epsilon$  is about  $+0.5$ , and  $\langle z^2 \rangle -$

Table 1. Quadrupole splitting and isomer shift for  $\text{Fe}^{57}$  at the surface of  $\eta$   $\text{Al}_2\text{O}_3$ .

Temp. ( $^\circ\text{K}$ )	Quadrupole splitting ( $2\epsilon$ ) (mm/sec)	Peak shift relative to $\text{Fe}^{57}$ in Cr (mm/sec)
300	$1.06 \pm 0.01$	$0.450 \pm 0.005$
77	$1.08 \pm 0.02$	$0.56 \pm 0.01$

$\langle x^2 \rangle \approx 1 \times 10^{-18} \text{ cm}^2$ . The positive sign of  $\epsilon$  means that the amplitude of vibration along the axis of the electric-field gradient, hence normal to the surface, is greater than the amplitude of vibration parallel to the surface. This is clearly plausible, although the published treatment of surface dynamics made use of too simple a model to predict (11). A more realistic model leads to the prediction of a sizable effect of this sort (12).

A measurement of the absolute Debye-Waller factor combined with this result would give  $\langle x^2 \rangle$  and  $\langle z^2 \rangle$  separately; such a measurement is quite difficult to make reliably, and we have not made it yet. The temperature shift of  $0.11 \text{ mm/sec}$  from  $77^\circ$  to  $300^\circ\text{K}$  is about the same as that for  $\text{Fe}^{57}$  in iron

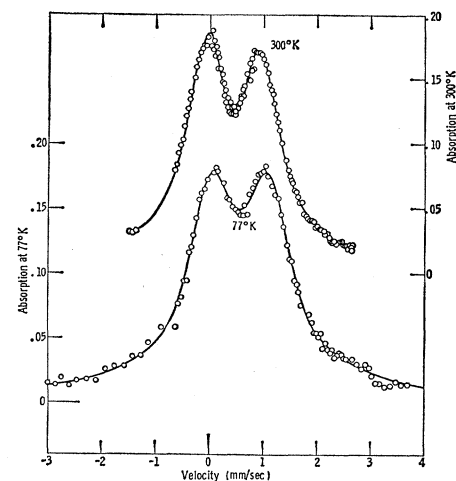


Fig. 1. Mössbauer absorption spectra for  $\text{Fe}^{57}$  at the surface of  $\eta$   $\text{Al}_2\text{O}_3$ .

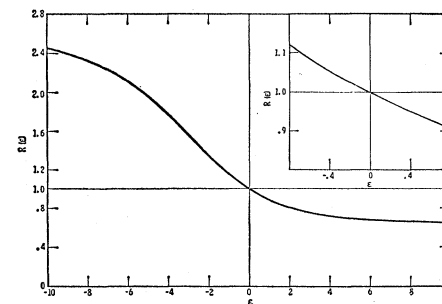


Fig. 2. Intensity ratio for a quadrupole split pattern as a function of the anisotropy of thermal vibration.

metal, indicating that the ions are bound with a comparable stiffness. A precise measurement of this shift as a function of temperature could be used to obtain quantitative information about this stiffness (13).

In general, it appears that the Mössbauer effect can readily be observed for atoms in surface sites of materials with high specific surface areas, and that it can be used to study both the chemical state and the dynamics of such atoms.

P. A. FLINN\*

S. L. RUBY

Westinghouse Research Laboratories,  
Pittsburgh 35, Pennsylvania

W. L. KEHL

Gulf Research and Development Corp.,  
Pittsburgh 30

#### References and Notes

1. D. S. Chapin and H. L. Johnston, *J. Am. Chem. Soc.* **79**, 2406 (1957); C. M. Cunningham and H. L. Johnston, *ibid.* **80**, 2377 (1958).
  2. H. C. Stumpf, A. S. Russell, J. W. Newsome, C. M. Tucker, *Ind. Eng. Chem.* **42**, 1398 (1950).
  3. G. Shirane, C. W. Chen, P. A. Flinn, R. Nathans, *Phys. Rev.* **131**, 183 (1963). For details of the apparatus, see P. A. Flinn, *Rev. Sci. Instr.* **34**, 1422 (1963).
  4. L. R. Walker, G. K. Wertheim, V. Jaccarino, *Phys. Rev. Letters* **6**, 98 (1961).
  5. V. I. Goldanskii, E. F. Makarov, V. V. Khrapov, *Phys. Letters* **3**, 344 (1963).
  6. H. M. Foley, R. M. Sternheimer, D. Tycko, *Phys. Rev.* **93**, 734 (1954).
  7. G. Burns, *ibid.* **124**, 524 (1961).
  8. C. F. Johnson, W. Marshall, G. J. Perlow, *ibid.* **126**, 9 (1962).
  9. G. K. Wertheim and D. N. E. Buchanan, in *The Mössbauer Effect*, Proc. 2nd Intern. Conf., D. M. J. Compton and A. H. Shoen, Eds. (Wiley, New York, 1962).
  10. S. De Benedetti, G. Lang, R. Ingalls, *Phys. Rev. Letters* **6**, 60 (1960).
  11. M. Rich, *Phys. Letters* **4**, 153 (1963).
  12. A. A. Maradudin and J. Melngailis, *Phys. Rev.* **133**, A1188 (1964).
  13. A. A. Maradudin, P. A. Flinn, S. Ruby, *Phys. Rev.* **126**, 9 (1962).
- We thank A. V. Fareri and M. M. Stewart for help in the preparation of the sample, and A. A. Maradudin for helpful discussion.
- \* Present address: Physics Department, Carnegie Institute of Technology, Pittsburgh 13, Pa.

30 October 1963

## Electrical and Thermal

### Measurements with Bridgman Anvils

**Abstract.** Multiple probe electrical and thermal measurements at high pressures can be made routinely with Bridgman anvils by using epoxide adhesive rings.

The use of Bridgman anvils (1) to attain high pressure is attractively simple, but the method has limited versatility. Success of this technique depends upon use of a ring, traditionally of pyrophyllite, that will contain the

sample and yet permit relative motion of the anvils so that the sample may be compressed. Since pyrophyllite is quite fragile and the ring must be very thin, electrical contact with the sample can be made only by the two anvils. Attempts have been made to use split rings to introduce additional leads into the pressure cavity but the technique is not an easy one (2). We have found that the substitution of an appropriate epoxide adhesive for pyrophyllite as the ring material increases greatly the versatility and usefulness of the Bridgman anvils. Rings made of epoxide are rugged, easy to prepare, possess excellent electrical properties, and make it very simple to introduce several additional leads. Since different metals may be used readily as leads, new experimental possibilities become available.

Eccobond 104 epoxide adhesive (3), a viscous liquid when initially prepared, is spread onto teflon blocks and cured in thin sheets (0.02 to 0.10 cm thick) from which the Bridgman gaskets are made by machining or punching. Such gaskets have been used in two standard geometries: anvil flat 0.65 cm, sample 0.35 cm and anvil flat 1.25 cm, sample 0.65 cm diameters.

Their suitability for high pressure work was tested by examining the I-II and III-IV transitions of bismuth embedded in silver chloride. With the smaller anvils the lower transition occurs at a nominal pressure (applied force divided by area of anvil flat) of 24 kb (currently accepted value 25.4 kb) and the higher bismuth transition at 80 kb. When KCN is used as the pressure medium the I-II transition occurs at about 20 kb. The relationship between the nominal pressure and the true pressure depends upon the nature, loading, and geometry of the sample. With gaskets made from an isotropic material (for example, epoxide adhesive) pressure multiplication is often found (4).

Electrical leads are introduced into the high pressure area by casting the leads directly in the epoxide. This is done by fixing a teflon pin on the teflon block, running wires from the pin, and spreading the epoxide over the wires and around the pin. After curing, the pin is removed, leaving a hole for the sample. The wires protruding into the hole are cut as desired. Chromel and alumel wires of 0.025 cm in diameter have proved satisfactory. It appears that metals which do not "cold work" too rapidly and have a high ductility are suitable as leads.

Figure 1 shows the resistance as a function of pressure for copper phthalocyanine. The measurements were made with leads brought out through the epoxide gasket. The change in  $d \log R/dP$  at a nominal pressure of 45 kb is associated with a phase transition (5).

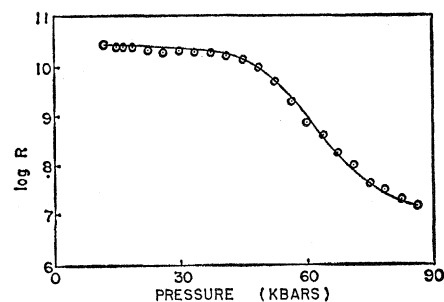


Fig. 1. Resistance of copper phthalocyanine as a function of pressure.

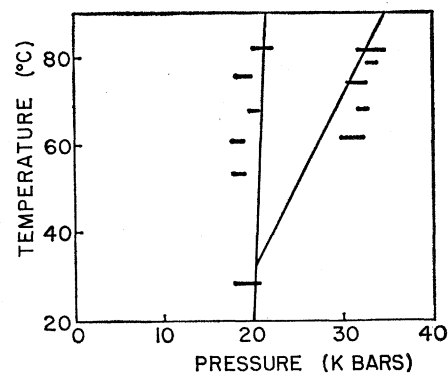


Fig. 2. Phase diagram of KCN determined by observing transition heats. Bridgman's results shown by solid line.

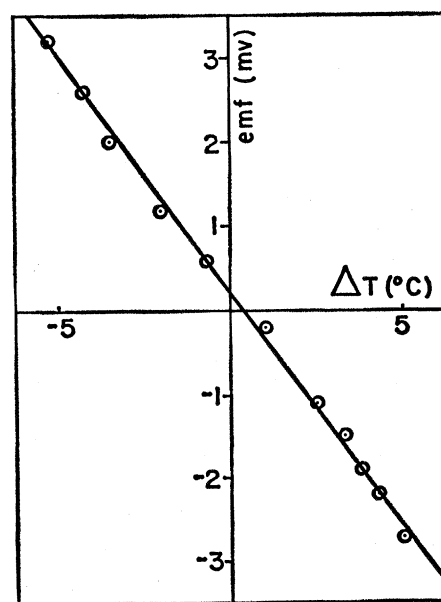


Fig. 3. The thermoelectric electromotive force of copper phthalocyanine at 20 kb.